A 3*M*-Device Cavity-Type Power Combiner

MOHAMMAD MADIHIAN, STUDENT MEMBER, IEEE, AND SHIZUO MIZUSHINA, MEMBER, IEEE

Abstract—**This paper describes a new class of combiners which combine the powers from $3M$ ($M=1,2,\cdots$) active devices by coupling them to both magnetic and electric fields inside a rectangular waveguide cavity. The structure employs coaxial lines and probes for magnetic and electric coupling, respectively. Up to 18 Gunn diodes have been combined with combining efficiencies higher than 96 percent at *X*-band. The operation of all combiners was stable and neither spurious oscillations nor jump phenomena were observed. An eigenfunction approach is used to analyze the operating principles of the combiner network systematically. A description is given to operate the circuit under optimum conditions.**

I. Introduction

In recent years, a variety of cavity-type power-combining structures have been reported which sum the outputs of N active devices in a single cavity and demonstrate high combining efficiency and satisfactory operation [1]–[6]. Nevertheless, it is desirable to develop new methods which increase the density of devices in a cavity-type power combiner, hence, the output power. Hamilton [7] has succeeded in increasing the number of devices combined per half guide wavelength in the Kurokawa oscillator. In his circuit a group of coaxial modules each containing an active device are placed symmetrically about the peak of the magnetic field. Similarly, Diamond [8] has suggested an approach to double the number of devices in the Harp and Stover circular cavity by coupling them to the magnetic field from both the top and bottom of the cavity.

In previous work, we reported on an oscillator circuit which couples active devices to both magnetic and electric fields inside a rectangular waveguide cavity [9]. The present paper uses this building-block circuit to develop a combining structure incorporating $3M$ active devices. The combining network is analyzed employing an eigenfunction approach in a form applicable to the treatment of non-uniform networks. Experimental results obtained from combiners with $M \leqslant 6$ are presented.

II. Principles of Operation

Fig. 1 shows a $3M$-device combiner. Active devices on the sides of a rectangular waveguide cavity are coupled to the magnetic field and those at the center are coupled to the electric field inside the cavity where the fields are maximum for the dominant TE_{10M} mode. Coupling is by means of coaxial lines and probes, respectively. The cavity is short circuited at one end, and coupled to a matched load through an inductive window at the other end. DC bias is applied to the side devices through the inner conductor of the coaxial lines, and to the center devices using thin wires connected to the probes inside the cavity.

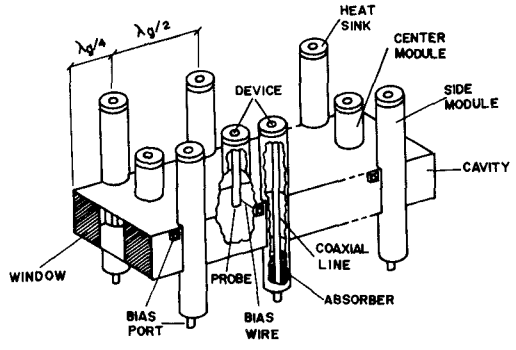

Fig. 1. The $3M$-device power combiner.

The structure can essentially be considered as a combination of the Kurokawa oscillator and probe-coupled oscillator. An equivalent circuit of this structure near each resonant frequency of the cavity is depicted in Fig. 2, where $3M$ identical devices represented by the impedance $-Z_d$ are coupled to a common cavity denoted by the parallel RLC circuit with R as cavity internal losses and $\omega_0 = 1/\sqrt{LC}$ as the resonant frequency. X_p is the series reactance of each probe, and the ideal input transformer $(n_g:1)$, $g=1,2,\cdots,M$, represents the electric coupling [10]. R_0 denotes the impedance of the flat-type absorbers seen from the cavity mid-height, and the ideal input transformer $(n_h:1)$, $h=M+1, M+2,\cdots,3M$, represents the magnetic coupling. Z_c, 1_E, and 1_H are the characteristic impedance and lengths of the coaxial sections in the center and side modules, respectively. The window is denoted by the ideal output transformer $(n_0:1)$, and R_L stands for the output load. The effects of the discontinuities introduced in the coaxial lines, probes, and cavity are incorporated into the parallel circuit indicating the cavity. The direct coupling between any pair of coaxial line-to-coaxial line, coaxial line-to-probe, and probe-to-probe is neglected.

The $3M$-port network is apparently non-uniform due to the existence of different series elements in each branch, i.e., jX_p, R_0, and the coaxial sections with different lengths. However, if we select the reference planes of the network at the terminals of the input transformers $(n_j:1)$, $j=1,2,\cdots,3M$, it is possible to make the network uniform,

Manuscript received November 2, 1982; revised May 3, 1983.

M. Madihian was with the Research Institute of Electronics, Shizuoka University, Hamamatsu 432, Japan. He is now with the Microelectronics Research Laboratories, Nippon Electric Co., Ltd., 4-1-1 Miyazaki, Miyamae-ku, Kawasaki 213, Japan.

S. Mizushina is with the Research Institute of Electronics, Shizuoka University, Hamamatsu 432, Japan.

0018-9480/83/0900-0731$01.00 ©1983 IEEE

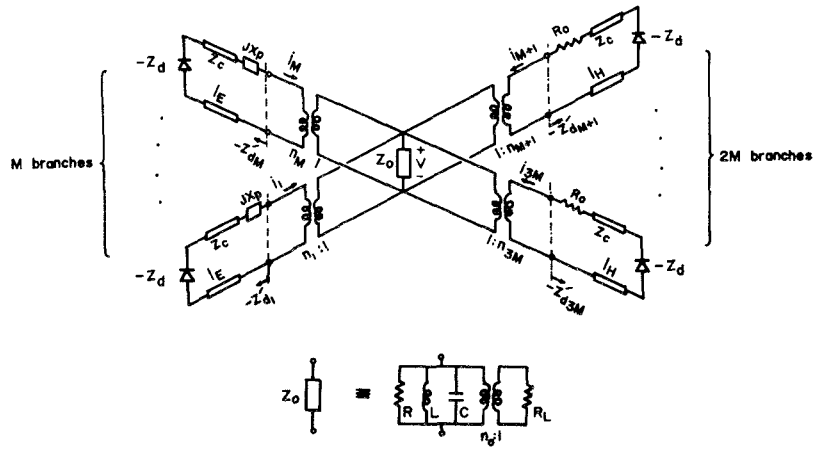

Fig. 2. Equivalent circuit of the $3M$-device power combiner.

and consequently, to apply an eigenfunction approach for a systematic analysis of the circuit.

The free-running oscillation condition for the $3M$-device oscillator, then, can be obtained from

$$(Z - Z_d')i = 0 \tag{1}$$

where i is the current vector with its component the RF current flowing into each port, and Z a $(3M \times 3M)$ impedance matrix representing the network

$$Z = Z_0 \begin{bmatrix} n_1^2 & n_1 n_2 & \cdots & n_1 n_{3M} \\ n_2 n_1 & n_2^2 & \cdots & n_2 n_{3M} \\ \cdot & \cdot & & \cdot \\ \cdot & \cdot & & \cdot \\ n_{3M} n_1 & n_{3M} n_2 & \cdots & n_{3M}^2 \end{bmatrix} \tag{2}$$

with

$$Z_0 = \sqrt{C/L}\left(j(\omega/\omega_0 - \omega_0/\omega) + 1/Q_0 + 1/Q_{\text{ext}}\right)^{-1},$$

$$Q_0 = R/L\omega_0, Q_{\text{ext}} = n_0^2 R_L/L\omega_0.$$

Z_d', on the other hand, is a diagonal matrix with its element the negative of the device impedance seen from each reference plane

$$-Z_{d1}' = -Z_{d2}' = \cdots = -Z_{dM}' = jX_p + Z_c \frac{-Z_d + jZ_c \tan(\beta l_E)}{Z_c - jZ_d \tan(\beta l_E)} \equiv -Z_{dE}' \tag{3}$$

$$-Z_{dM+1}' = -Z_{dM+2}' = \cdots = -Z_{d3M}' = R_0 + Z_c \frac{-Z_d + jZ_c \tan(\beta l_H)}{Z_c - jZ_d \tan(\beta l_H)} \equiv -Z_{dH}' \tag{4}$$

where β is the propagation constant of the coaxial sections. Unless otherwise stated, it is assumed that (3) and (4) are made equal, i.e., $-Z_{dE}' = -Z_{dH}' \equiv -Z'$, by proper selection of l_E and l_H.

The eigenvectors X and associated eigenvalues λ for the matrix Z are given by

$$X_0 = \begin{bmatrix} n_1 \\ n_2 \\ \cdot \\ \cdot \\ n_{3M} \end{bmatrix} \qquad X_m = \begin{bmatrix} 1/n_1 \\ \exp(jma)/n_2 \\ \cdot \\ \cdot \\ \exp(jm(3M-1)a)/n_{3M} \end{bmatrix} \tag{5}$$

and

$$\lambda_0 = bZ_0 \qquad \lambda_m = 0 \tag{6}$$

respectively, where $a = 2\pi/3M$, $m = 1, 2, \cdots, 3M-1$, and $b = n_1^2 + n_2^2 + \cdots + n_{3M}^2$.

In regard to a discussion presented in [11], possible solutions to the port currents are given by

$$i = X_k \tag{7}$$

provided that

$$Z_d' = \lambda_k I \tag{8}$$

where $k = 0, 1, 2, \cdots, 3M-1$, and I is the identity matrix. With respect to (7) and (8), there are altogether $3M$ modes of oscillation for each resonant mode of the cavity. The eigenvector X_0 and associated eigenvalue λ_0 correspond to the desired in-phase mode of the combiner, while X_m and λ_m are associated with anti-phase modes of no RF output.

III. Desired Mode of Oscillation

For the desired mode of oscillation, except for a possible difference in the sign, all the coaxial lines see the same magnetic-field configuration, and all the probes see the same electric-field configuration

$$n_1^2 = n_2^2 = \cdots = n_M^2 \equiv n_E^2 \tag{9}$$

$$n_{M+1}^2 = n_{M+2}^2 = \cdots = n_{3M}^2 \equiv n_H^2. \tag{10}$$

Hence, the port current and oscillation condition will be, respectively, given by

$$i = \begin{bmatrix} n_E \\ \cdot \\ \cdot \\ n_E \\ n_H \\ \cdot \\ \cdot \\ n_H \end{bmatrix} \begin{matrix} \} M \\ \\ \\ \\ \} 2M \\ \\ \\ \end{matrix} \tag{11}$$

and

$$Z' = M(n_E^2 + 2n_H^2)Z_0. \tag{12}$$

It is worth noting that despite the device impedances $-Z'$ presented to all the ports are identical, the currents are different by the factor n_E/n_H. This physically reflects the fact that a part of the power generated by the side devices

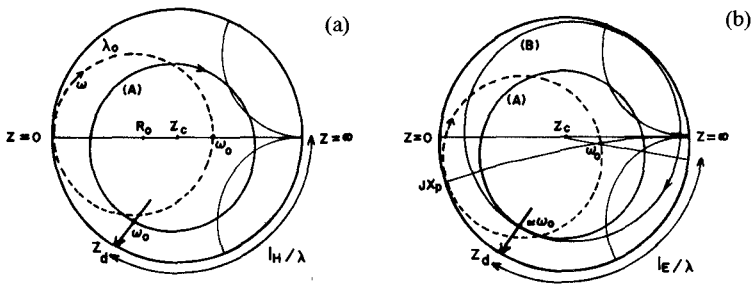

Fig. 3. Graphic realization of oscillation condition for the $3M$-device combiner. (a) Side modules. (b) Center modules.

is dissipated in the respective resistor R_0. Therefore, the net power delivered to each transformer $(n_H:1)$ is less than the power delivered to each transformer $(n_E:1)$.

A graphic realization of the oscillation condition for two different branches representing the side and center modules is shown in Fig. 3. Let us suppose that the actual device line Z_d is located as shown in the figure. We note that

$$\lambda_0 = n_j V/i_j, \qquad j=1,2,\cdots,3M$$

where

$n_j \equiv$ the turn ratio of the transformer of the j-th port,
$V \equiv$ the voltage developed across Z_0, and
$i_j \equiv$ the current flowing into the j-th port.

Therefore, the locus of λ_0 varies in the Smith chart as represented by the dotted circle in Fig. 3(a). Adding R_0 to this circle and rotating the new locus by an electrical length $2\pi l_H/\lambda$, one can obtain circle (A) which represents the impedance locus seen by the side devices. Similarly for the center devices, by adding jX_p to λ_0, we obtain the dotted circle shown in Fig. 3(b). Then rotating this circle by an electrical length $2\pi l_E/\lambda$ and adjusting the electric coupling, in effect n_E, one plots circle (B) which can coincide with (A) in the vicinity of the cavity resonant frequency ω_0. Finally, by proper selection of the window width, effectively n_0, the diameters of the two loci, hence, the operating point on the device line Z_d can be adjusted for maximum output power.

Stability conditions for the desired mode of oscillation are the same as those derived by Kurokawa for his circuit [1].

IV. Undesired Modes of Combiner

There are two different phenomena which may bring about mode instabilities. One has to do with higher resonant modes of the cavity and the other is associated with different modes of oscillation for each resonant mode of the cavity.

Due to the existence of the absorbers, there is no coupling between the side modules and the cavity at higher resonant modes [1]. On the other hand, the next higher cavity mode which couples to the probes in the center modules is TE_{30M} mode. However, the cutoff frequency of this mode is 19.6 GHz, hence, outside the frequency range over which the devices exhibit a negative resistance. Fig. 4 shows a picture of the circuit impedance $jX_p + \lambda_0$, corresponding to the dotted circle in Fig. 3(b), measured over a frequency range of 6.7–18 GHz. The measurement assumes

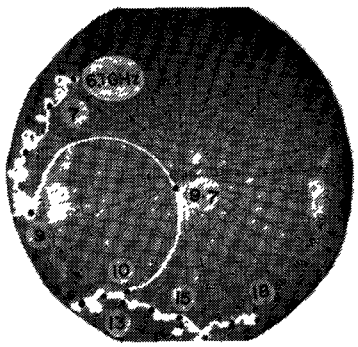

Fig. 4. A picture of the circuit impedance seen by the probes in the center modules over a frequency range of 6.7–18 GHz.

the probe's input terminal as the reference plane. The locus forms a circle representing the coupling between the probe and the cavity in the vicinity of the resonant frequency of 9.7 GHz, and stays at the periphery of the chart at other frequencies. With these observations, one may conclude that the possibility of having oscillations at frequencies removed from the dominant resonant frequency can be practically eliminated for this combiner.

On the other hand, for the dominant resonant mode of the cavity, there are $3M-1$ undesired modes of oscillation. With respect to (6) and (8), the combiner will oscillate in these modes if

$$Z_d' = \lambda m I = 0, \qquad m=1,2,\cdots,3M-1. \tag{13}$$

Expressing (13) in terms of the circuit elements in the side and center modules, respectively, one can write the following two equations:

$$Z_d = Z_c \frac{R_0 + jZ_c \tan(\beta 1_H)}{Z_c + jR_0 \tan(\beta 1_H)} \equiv Z_H \tag{14}$$

$$Z_d = Z_c \frac{jX_p + jZ_c \tan(\beta 1_E)}{Z_c - X_p \tan(\beta 1_E)} \equiv Z_E. \tag{15}$$

Equations (14) and (15), respectively, state that in the $3M-1$ undesired modes of oscillation, each side device observes the impedance R_0 transformed by an electrical length $2\pi 1_H/\lambda$, and each center device sees the reactance X_p transformed by an electrical length $2\pi l_E/\lambda$. Therefore, the combiner can be prevented from oscillating in undesired modes so long as $Z_d \neq Z_H$ and $Z_d \neq Z_E$. These conditions have been achieved in the actual circuit by choosing the lengths l_H and l_E, in order to obtain an optimum operation in the desired mode.

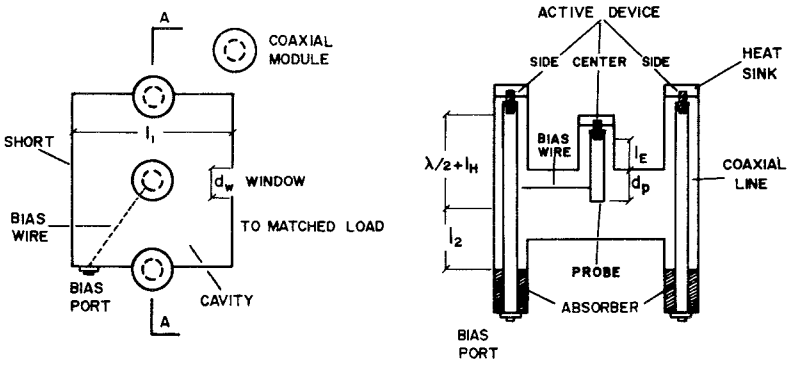

(a) (b)

Fig. 5. Configuration of the 3-device building-block structures. (a) Top view. (b) Cross-sectional view at AA.

We did not observe any oscillation related to either higher resonant modes of the cavity or undesired modes of oscillation during the circuit adjustments using Gunn diodes, which, generally, exhibit negative resistance over, say, a frequency range of 7–15 GHz.

V. Output Power and Circuit Efficiency

To calculate the output power and circuit efficiency of the combiner, we assume that the oscillation frequency is approximately equal to the resonant frequency of the cavity, and losses of the coaxial sections are negligible. The combined power delivered to the load is thus given by

$$P_c = \frac{R}{R + n_0^2 R_L} P \tag{16}$$

where P, the power presented to Z_0, is equal to

$$P = M(P_E + 2P_H). \tag{17}$$

P_E and P_H are the power contributed by each center and side device, respectively, at the reference planes. Thus

$$P_E = P_g \tag{18}$$

and

$$P_H = \left(1 - \frac{R_0}{\mathrm{Re}\{Z_d\}}\right) P_g \tag{19}$$

where P_g is the power generated by an individual device. Inserting (17)–(19) into (16), one can write

$$P_c = 3M\left(\frac{1}{1 + Q_{\mathrm{ext}}/Q_0}\right)\left(1 - \frac{2R_0}{3\,\mathrm{Re}\{Z_d\}}\right) P_g. \tag{20}$$

The circuit efficiency of the combiner is, therefore, equal to

$$\eta_c = \frac{P_c}{3M \cdot P_g} = \left(\frac{1}{1 + Q_{\mathrm{ext}}/Q_0}\right)\left(1 - \frac{2R_0}{3\,\mathrm{Re}\{Z_d\}}\right) \tag{21}$$

which is larger than that of the Kurokawa oscillator [1].

VI. Experiments

The validity of the descriptions given for the $3M$-device combiner has already been experimentally verified using 3-device oscillators [10]. The experiments carried out here increase the total number of devices up to 18 ($M = 6$), by cascading pretuned 3-device building-block structures as shown in Fig. 5.

TABLE I
Circuit Parameters and Performance Data of the 3-Device Structures

Osc. No.	l_1 (mm)	l_2 (mm)	l_E (mm)	l_H (mm)	d_p (mm)	d_w (mm)	P_E (mW)	$2P_H$ (mW)	P_o (mW)	f (MHz)	Δf (MHz)	Q_{ext}
1	19	16	7.5	8	2.5	7.1	22	43	60	9790	32	194
2	19	16	7.5	8	2.5	7.4	23	41	62	9770	33	189
3	19	16	7.5	8	2.5	7.1	20	44	66	9790	32	194
4	19	16	7.5	8	2.5	8.4	21	44	67	9780	36	170
5	19	16	7.5	8	2.5	6.1	24	42	68	9800	30	207
6	19	16	7.5	8	2.5	7.9	25	45	69	9785	34	180

The 3-device structures were constructed using standard rectangular waveguides (22.9 mm×10.2 mm) and Gunn diodes (NEC GD 511 AA), in the following manner. First the side devices were mounted at one end of 50-Ω coaxial lines and a circuit adjustment was made to find the appropriate position of the devices, as well as the absorbers (ECCOSORB), using a proper window. Then, the center device was mounted at one end of a 50-Ω coaxial transformer with a proper length, and the other end of the transformer was extended into the cavity as a probe. Finally, the window width was readjusted to obtain the sum of the powers from three devices. It is worth noting that readjustment of the flat-type absorbers, which provide an additional degree of freedom in circuit tuning, improved the output power level by approximately 5 percent. The circuit parameters and performance data of the 3-device building-block structures are listed in Table I. P_E and $2P_H$ are the output power if the 3-device structures contain only the center device or two side devices, respectively. P_o is the output power with all three devices operating. Due to small differences among the devices, the optimum window width is not the same for all the structures.

$3M$-device combiners were built by stacking first M structures in Table I and using appropriate windows. Moreover, we applied thin waveguide sections to adjust the space between two adjacent structures for maximum combined output power P_c. Optimum spacing S was found to be 0.5 mm $\leqslant S \leqslant$ 1.5 mm, for $2 \leqslant M \leqslant 6$. Results of such power combining are shown in Table II where η, the combining efficiency, is defined as the ratio of P_c to the sum of the output powers from the structures cascaded. As Table II shows, combining efficiencies greater than 96

TABLE II
RESULTS OF POWER COMBINING FOR $M = 2,3,\cdots,6$

No. of struc.s cascaded M	No. of devices combined 3M	d_w (mm)	P_c (mW)	f_c (MHz)	η (%)	Δf (MHz)	Q_{ext}
2	6	9	120	9800	99	47	132
3	9	9.5	184	9806	98.1	57	110
4	12	9.8	248	9808	97.5	65	95
5	15	10.1	314	9815	97.4	70	90
6	18	10.4	377	9820	96.2	74	84

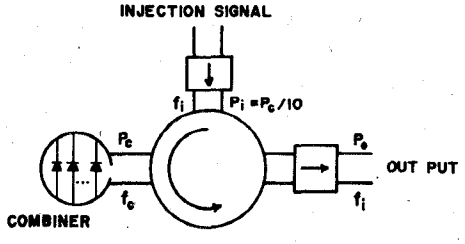

Fig. 6. Arrangement for injection locking of the $3M$-device structures.

percent are obtained for all the cases of $M \leqslant 6$. The operation of all the combiners was stable and neither spurious oscillations nor jump phenomena were observed during the experiments.

The effect of cavity tuning on the operation of the circuits was examined using a moveable short; the 3×6-device combiner could be tuned over 400 MHz with 0.4-dB power variation. This implies that tuning of the cavity causes the same frequency changes on the two loci (A) and (B), Fig. 3. The circuit efficiency of the structures was compared to that of the Kurokawa oscillator. With respect to Table II, the output power obtained from the 3×6-device combiner was 377 mW. On the other hand, maximum output power obtained from an 18-device Kurokawa oscillator using the same devices was 362 mW. This indicates an average of 3.7-percent improvement in the output power level, due to the existence of fewer absorbers in the 3×6-device circuit.

We also examined the injection-locking behavior of the $3M$-device structures using the setup of Fig. 6. First the circuit was adjusted for maximum output power. Then, an injection signal providing a gain of 10 dB was applied to the combiner and locking bandwidth Δf was measured by sweeping the injection frequency. The external Q, Q_{ext}, of the structures, calculated from bandwidth measurement, is also presented in the tables.

VII. CONCLUSIONS

A new class of cavity-type power combiners was introduced which incorporates $3M$ active devices in a single cavity by means of both magnetic and electric coupling mechanisms. A method for systematic analysis of the combiner network was developed which can be applied to treat non-uniform combining structures. Up to 18 Gunn diodes were combined at X-band to verify the validity of the theoretical analysis. Based on the procedure established by the analysis, the circuit parameters were adjusted to obtain the sum of the powers from individual devices. Combining efficiencies achieved were higher than 96 percent. Injection-locking experiment with the $3M$-device oscillators has shown an increasing locking bandwidth with the number of devices combined. The combining structure developed is hoped to find application in millimeter-wave bands, since it adds a third device per half guide wavelength to the Kurokawa oscillator, which has been successfully applied to these bands.

REFERENCES

[1] K. Kurokawa, "The single-cavity multiple-device oscillator," *IEEE Trans. Microwave Theory Tech.*, vol. MTT-19, pp. 793–800, Oct. 1971.
[2] R. S. Harp and H. L. Stover, "Power combining of X-band IMPATT circuit modules," in *Proc. 1973 IEEE Int. Solid-State Circuit Conf.*, Feb. 1973.
[3] K. Chang and R. L. Ebert, "W-band power combining design," *IEEE Trans. Microwave Theory Tech.*, vol. MTT-28, pp. 295–305, Apr. 1980.
[4] M. Dydyk, "Efficient power combining," *IEEE Trans. Microwave Theory Tech.*, vol. MTT-28, pp. 755–762, July 1980.
[5] S. Nogi and K. Fukui, "Optimum design and performance of a microwave ladder oscillator with many diode mount pairs," *IEEE Trans. Microwave Theory Tech.*, vol. MTT-30, pp. 735–743, May 1982.
[6] K. J. Russell, "Microwave power combining techniques," *IEEE Trans. Microwave Theory Tech.*, vol. MTT-27, pp. 472–478, May 1979.
[7] S. E. Hamilton and B. M. Fish, "Multidiode waveguide power combiners," in *Proc. 1982 IEEE Microwave Theory Tech. Symp.*, June 1982.
[8] F. Diamond, "Ku band power combining of push-pull operated IMPATT diodes," in *Proc. 1979 European Microwave Conf. Dig.*, pp. 566–570.
[9] M. Madihian, A. Materka, and S. Mizushina, "A multiple-device cavity oscillator using both magnetic and electric coupling mechanisms," *IEEE Trans. Microwave Theory Tech.*, vol. MTT-30, Nov. 1982.
[10] R. F. Harrington, *Time-Harmonic Electromagnetic Fields.* New York: McGraw-Hill, 1961, pp. 434–436.
[11] K. Kurokawa, "An analysis of Rucker's multidevice symmetrical oscillator," *IEEE Trans. Microwave Theory Tech.*, vol. MTT-18, pp. 967–969, Nov. 1970.

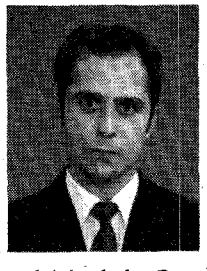

Mohammad Madihian (S'78) was born in Tehran, Iran, on January 3, 1954. He received the B.Sc. degree from the Iran College of Science and Technology, Tehran, Iran, in 1976, and the M.Sc. and Ph.D. degrees from Shizuoka University, Hamamatsu, Japan, in 1980 and 1983, respectively, all in electronic engineering.

From 1976 to 1977 he was with the Azad University of Iran, Tehran, Iran, serving as a Research Assistant. In 1977 he won a Japanese Ministry of Education (Monbusho) Scholarship and joined the Research Institute of Electronics, Shizuoka University, Hamamatsu, Japan, where he has worked on research and development of phase-sensitive detectors, phase filters, microwave solid-state oscillators, and power combiners. He is currently with the Microelectronics Research Laboratories, Nippon Electric Company, Kawasaki, Japan, working on research and development of microwave monolithic GaAs FET oscillator circuits.

Dr. Madihian is a member of the Institute of Electronics and Communication Engineers of Japan.

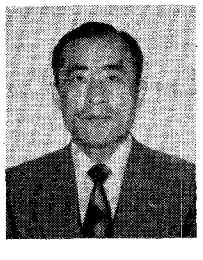

Shizuo Mizushina (S'60–M'66) was born in Hamamatsu, Japan, on August 10, 1933. He received the B.Eng. degree from Shizuoka University, Hamamatsu, in 1957, and the M.Sc. and Ph.D. degrees from The Ohio State University, Columbus, in 1962 and 1964, respectively.

From 1957 to 1960 he was a Research Assistant and Lecturer at Shizuoka University. From 1964 to 1965 he was a member of the Technical Staff at the Bell Telephone Laboratories, Murray Hill, NJ. In 1965 he returned to Shizuoka Uni-

versity where he is a Professor at the Research Institute of Electronics. He has worked on milimeter-wave magnetrons, gigabit-pulse regenerators, solid-state oscillators, and device-circuit interaction problems. His current research interests are concerned with microwave power-combining techniques, microwave thermography, and medical electronics.

Dr. Mizushina is a member of the Institute of Electronics and Communication Engineers of Japan, the Japan Society of Medical Electronics and Biological Engineering, and Sigma Xi.

Transversely Anisotropic Optical Fibers: Variational Analysis of a Nonstandard Eigenproblem

ISMO V. LINDELL, SENIOR MEMBER, IEEE MARKKU I. OKSANEN, STUDENT MEMBER, IEEE

Abstract—**The variational principle for nonstandard eigenvalue problems, recently reported by one of the authors, is applied for the study of guided-wave propagation in an anisotropic dielectric waveguide. A stationary functional is derived for the general dielectric waveguide with transverse anisotropy. The functional is tested for the well-known case of an isotropic step-index single-mode fiber. It is seen that for simple trial functions with only two parameters, a good accuracy is obtained. For two types of transversely anisotropic step-index fibers, relations between the propagation factor, anisotropy parameter, dielectric parameter, and frequency are calculated. The functional does not assume weak guidance condition nor perturbational anisotropy and, hence, is also applicable for other dielectric waveguides. In this application, only a modest computer or a programmable calculator is needed. Moreover, the spurious modes causing confusion in the finite-element method of calculation do not appear with the present method.**

I. Introduction

THE OPTICAL FIBER has become one of the most studied subjects in electromagnetics because of its phenomenological property of wave guidance with extremely low losses. In recent years, the single-mode fiber has been favored because of its small dispersion, but the problem has been the degeneracy in the polarization of the basic HE_{11} mode in fibers with circular symmetry. Because of this, the small imperfections in the ambient conditions of the fiber have the effect of making the polarization of the mode a statistically varying quantity after a few meters of propagation in the fiber [1]–[5], a fact that has been counteracted by producing noncircular or transversely anisotropic fibers. By analysis and actual fabrication, it has been shown that the noncircularity in most cases is insufficient to produce the required separation of the polarization degenerate mode propagation coefficients, whereas by introducing mechanical stress in the fiber, an anisotropy can be obtained high enough to produce a separation sufficient in practice [3], [6]–[17]. This motivates an analysis of the dielectric waveguide with transverse anisotropy, because although the longitudinal anisotropy has been well studied [18]–[21], there only exist a few attempts with more general anisotropy: mainly perturbational or dealing with special structures [22]–[26].

The analysis applies the variational principle in the general eigenvalue problem which was called nonstandard in a recent study by one of the authors [27]. Here, the problem can be expressed in abstract operator form as

$$L(\lambda)f = 0 \tag{1}$$

where λ is the eigenvalue parameter of the problem. If $L(\lambda)$ is a linear function on λ, (1) is a standard eigenvalue problem, otherwise it is called nonstandard. The parameter λ may be chosen at will among all the physical and geometrical parameters involved in the problem. In problems dealing with closed waveguides, there is an additional equation corresponding to boundary conditions, which, however, is absent in our present problem. The method is based on the following functional equation obtained through definition of an inner product (...,...):

$$(f, L(\lambda)f) = 0. \tag{2}$$

If the operator L is self adjoint with respect to this inner product, it was shown that (2) possesses stationary roots for the parameter λ [27]. If we can solve (2) for λ, a stationary functional for λ is obtained, which can be applied for an approximative solution of the problem (1) in a well-known manner [28]. In more complicated problems, however, no explicit solution of (2) for the parameter λ can be found. In this case, we may try to take another parameter of the problem as our eigenvalue parameter λ. If none

Manuscript received November 12, 1982; revised May 3, 1983. This work was supported by a grant from the Academy of Finland.

The authors are with the Electrical Engineering Department, Helsinki University of Technology, Otakaari 5A, Espoo 15, Finland 02150.

0018-9480/83/0900-0736$01.00 ©1983 IEEE